CrystEngComm

View Online
Dynamic Article Links

Cite this: DOI: 10.1039/c1ce05196b

www.rsc.org/crystengcomm

PAPER

Three novel indium MOFs derived from diphenic acid: synthesis, crystal structures and supramolecular chemistry†

Ana E. Platero-Prats,[a] María C. Bernini,[ac] Manuela E. Medina,[a] Elena López-Torres,[ab] Enrique Gutiérrez-Puebla,[a] M. Ángeles Monge*[a] and Natalia Snejko[a]

Received 11th February 2011, Accepted 28th April 2011
DOI: 10.1039/c1ce05196b

Three In(III) MOFs based on diphenic acid and nitrogen-donor ancillary ligands were obtained as pure phases. Two of them have 1D chain structures, and the third forms 2D zig-zag layers. The different torsion angles adopted by the diphenic ligand along with the existence of several non-covalent interactions govern the crystal packing and determine the formation of a centrosymmetric one-dimensional compound (**1**) or a non-centrosymmetric helical chain-based compound (**3**). Reaction with 2,2′-bipyridyl under certain conditions leads also to the formation of two dimeric precursors (compounds **4** and **5**). The topological study of all their nets is reported.

Introduction

The studies of Metal–Organic Frameworks (MOFs) resulted in some very fruitful researches in recent years, motivated by their potential applications as functional materials in selective adsorption and separation of organic molecules,[1–5] molecular recognition,[6,7] magnetism,[8–11] gas separation and storage,[12,13] catalysis,[14,15] *etc.* In the design and synthesis of desirable MOFs, the properties of the organic ligands play an important role: even small changes in flexibility, functional group position, length, and symmetry of the ligands can result in remarkably different materials with diverse architectures and properties.[16]

Due to their versatile coordination modes, rigid organic dicarboxylic acids are often used as bridging ligands to construct MOFs, as the organic component in such framework compounds.[16–19] On the other hand, flexible aromatic carboxylate ligands have attracted notably less attention. In our group we have previously obtained several MOFs based on the flexible V-shaped H_2hfipbb acid ((hexafluoroisopropylidene)bis(benzoic)acid).[20,21] As a continuation of this work, now we are interested in the use of diphenic acid (biphenyl-2,2′-dicarboxylic acid, H_2dpa from now on)[22–26] as ligand, due to the fact that it can be considered as a semi-rigid angular building block giving rise to diverse topologies, this feature being the opposite of the extensively used isomeric biphenyl-4,4′-dicarboxylic acid. On the other hand, the structural complexity and functional potential of dicarboxylate-containing coordination polymers can be elevated through the incorporation of neutral ancillary ligands such as 2,2′-bipyridine, 4,4′-bipyridine and phenanthroline.[27]

Whereas for transition metals and lanthanides plenty of coordination polymers have been reported, MOFs incorporating the IIIA group trivalent elements like In(III) ion have attracted less attention.[28] In our research group, we have been engaged in the design of indium MOFs, which have been proved to be active as Lewis and redox heterogeneous catalysts.[29–31] In this way and exploring the H_2dpa coordination capability with an In ion in the presence of aromatic ancillary amines, we report in this paper the synthesis, structure and characterization of three novel indium mixed-ligand MOFs, as well as the formation of two dimeric precursors built up from H_2dpa and ancillary ligands. Moreover, taking into account the supramolecular interactions found in these compounds, the topology of the nets of these In *frameworks* is also studied.

Experimental section

General information

All reagents were commercially available from Aldrich and were used as received. The IR spectra were recorded on a Jasco FT/IR-410 spectrophotometer as KBr pellets in the 4000–400 cm^{-1} range. Thermogravimetric analysis (TGA) was performed using a seiko TG/DTA 320 apparatus in a temperature between 25 and 800 °C under N_2 (flow of 50 mL min^{-1}) with a heating rate of 5 °C min^{-1}. Microanalyses were performed at the Microanalyses Service of the Universidad Autónoma de Madrid.

[a]*Instituto de Ciencia de Materiales de Madrid, CSIC, Sor Juana Inés de la Cruz, 3, Cantoblanco, 28049, Madrid, Spain. E-mail: amonge@icmm.csic.es; Fax: +34 91 372 0623; Tel: +34 91 334 9000*
[b]*Universidad Autónoma de Madrid, Cantoblanco, 28049, Madrid, Spain*
[c]*Área de Química General e Inorgánica "Dr G.F. Puelles" Facultad de Química, Bioquímica y Farmacia, Chacabuco y Pedernera, Universidad Nacional de San Luis, 5700 San Luis, Argentina*

† Electronic supplementary information (ESI) available. CCDC reference numbers 812721–812725. For ESI and crystallographic data in CIF or other electronic format see DOI: 10.1039/c1ce05196b

General synthesis procedure

$[In_2(L)_3(phen)_2]\cdot H_2O$ (1). A mixture of $In(OAc)_3$ (0.100 g, 0.34 mmol), diphenic acid, H_2L, (0.179 g, 0.7 mmol) and 1,10-phenanthroline monohydrate (0.068 g, 0.34 mmol) in 8 mL of distilled water was sealed in a Teflon-lined autoclave and heated at 170 °C for 20 h. After cooling to room temperature the colorless crystals formed were filtered off and washed with distilled water, ethanol and acetone. Yield: 0.147 g, 65%. Elemental analysis, found (calculated): C, 59.43 (59.66), H, 3.20 (3.19), N, 4.04 (4.22). IR (KBr, cm^{-1}): 3234 ν(OH), 3120 ν(C–H) phen, 3065 ν(C–H)L, 1602 ν(OCO)as, 1583 ν(C=N)phen, 1432 ν(OCO)s, 1398 ν(CC)as, 1153, 1106 ν(CC)s, 869, 849 δ_{oop}(C–H) phen, 760, 725, 688 δ_{oop}(C–H)L.

$[In_2(L)_2(4,4\text{-bipy})(OH)_2]\cdot 0.25H_2O$ (2). This compound was obtained by a similar procedure to the above described but using a mixture of $In(OAc)_3$ (0.300 g, 1 mmol), H_2dpa (0.245 g, 1 mmol), and 4,4′-bipyridyl (0.080 g, 0.54 mmol) in 15 mL of distilled water. The mixture was heated in a Teflon-lined autoclave at 150 °C for 20 h. After cooling to room temperature the colorless crystals formed were filtered off and washed with distilled water, ethanol and acetone. Yield: 0.343 g, 73%. Elemental analysis, found (calculated): C, 49.34 (49.66), H, 3.32 (3.05), N, 2.86 (3.05). IR (KBr, cm^{-1}): 3599 ν(OH), 3114 ν(C–H) bipy, 3071, 3052 ν(C–H)L, 1615 ν(OCO)as, 1598, 1582 ν(C=N) bipy, 1445 ν(OCO)s, 1408 ν(CC)as, 1154, 1112 ν(CC)s, 879, 815 δ_{oop}(C–H)bipy, 751, 723, 707 δ_{oop}(C–H)L.

$[In(L)(HL)(2,2'\text{-bipy})]\cdot 1/2H_2O$ (3). The synthesis procedure to obtain this compound is similar to that described for compounds **1** and **2** but in this case, a mixture of $In(OAc)_3$ (0.300 g, 1 mmol), H_2dpa (0.498 g, 2.05 mmol), and 2,2′-bipyridyl (0.159 g, 1.07 mmol) in 15 mL of distilled water was sealed in a Teflon-lined autoclave and heated at 150 °C for 20 h. The obtained colorless crystals formed after cooling to room temperature were filtered off and washed with distilled water, ethanol and acetone. Yield 0.539 g, 69%. Elemental analysis, found (calculated): C, 59.94 (59.60), H, 3.44 (3.41), N, 3.68 (3.5). IR (KBr, cm^{-1}): 3596, 3518 ν(OH)water, 3429, 3224 ν(OH)LH, 3114 ν(C–H)bipy, 3061 ν(C–H)L, 1729, ν(C=O), 1600 ν(OCO)as, 1583 ν(C=N)bipy, 1444, 1415 ν(OCO)s, 1374 ν(CC)as, 1162, 1131 ν(CC)s, 871, 805 δ_{oop}(C–H)bipy, 764, 733, 719, 688 δ_{oop}(C–H)L.

The purity of complexes **1–3** was also checked by comparison of their respective XRD powder patterns with the simulated ones from single-crystal X-ray diffraction data (see ESI, Fig. S1–S3†).

During the optimization of the synthesis conditions to obtain the previous compounds as pure phases, two additional compounds were found. These new phases, named compounds **4** and **5** from now on, were obtained always in a mixture with the compound **3**. In this way, we present here the synthesis conditions for obtaining such mixture. While compound **3** has been obtained pure in the previously described conditions, compounds **4** and **5** have not been isolated as pure phases. However, structural and topological studies are reported for both of them.

$[In_2(L)_2(HL)_2(2,2'\text{-bipy})_2]\cdot H_2O$ (4) and $[In_2(L)_2(HL)_2(2,2'\text{-bipy})_2]$ (5). A mixture of $In(OAc)_3$ (0.100 g, 0.34 mmol), H_2dpa (0.085 g, 0.35 mmol) and 2,2-bipyridyl (0.053 g, 0.35 mmol) in 8 mL of distilled water was sealed in a Teflon-lined autoclave and heated at 170 °C for 20 h. After cooling to room temperature the colorless crystals formed were filtered off and washed with distilled water, ethanol and acetone. Two types of crystals were obtained and were separated manually although both compounds could not be selectively synthesized.

X-Ray structure determination. Table 1 summarizes the main crystal and refinement data for the five compounds (Tables S1–S5 in the ESI† show the complete information of the single-crystal XRD data for **1–5**, respectively). Crystals were selected under a polarizing optical microscope and glued on a glass fiber for a single-crystal X-ray diffraction experiment. X-Ray intensity data were collected on two different equipments: a Bruker SMART CCD diffractometer and a Bruker four circle kappa-diffractometer. Single crystal XRD data for compounds **1**, **3–5** were collected using the first one, which is equipped with a normal focus, 2.4 kW sealed tube X-ray source (MoK_α radiation = 0.71073 Å). Data were collected at room temperature over a hemisphere of the reciprocal space by a combination of three sets of exposures. Each exposure of 10 s covered 0.3° in ω. An appropriate single crystal of the compound **2** was mounted on the Bruker four circle kappa-diffractometer equipped with a Cu INCOATEC microsource, operated at 30 W power (45 kV, 0.60 mA) to generate Cu Kα radiation (λ = 1.54178 Å), and a Bruker AXIOM area detector (microgap technology). Diffraction data were collected exploring over a hemisphere of the reciprocal space in a combination of π and ω scans to reach a resolution of 0.86 Å, using a Bruker APEX2 software suite (each exposure of 10 s covered 0.5° in ω).

Unit cell dimensions were determined by a least-squares fit of reflections with $I > 2\sigma(I)$. Data were integrated and scaled using SAINTplus program.[32] A semi-empirical absorption and scale correction based on equivalent reflection was carried out using SADABS.[32] Space group determinations were carried out using XPREP.[33] The structures were solved by direct methods. The final cycles of refinement were carried out by full-matrix least-squares analyses with anisotropic thermal parameters for all non-hydrogen atoms. Hydrogen atoms of the organic ligands were situated at their calculated positions. Calculations were carried out with SMART software for data collection and data reduction and SHELXTL.[34]

Results and discussion

Crystal structures

Compound 1. This compound crystallizes in the triclinic system, $P\bar{1}$ space group. The asymmetric unit consists of two independent In(III) ions, three types of diphenic ligands completely deprotonated ($C_{14}O_4H_8$) (L1A, L1B and L1C, from now on), two phenanthroline molecules and two hydration water molecules. It is possible to define two different coordination environments for In(III) ions in this compound: In(1) is octa-coordinated –[InO_6N_2]– with six In–O bonds coming from chelating carboxylate groups of L1 ligands and two In–N bonds coming from phenanthroline ligands which are bounded to In(1) in a chelate mode (see Fig. 1a). The resultant polyhedron is a triangulated dodecahedron. In(2) is heptacoordinated

Table 1 Main crystallographic data for compounds **1–5**

	Compound **1**	Compound **2**	Compound **3**	Compound **4**	Compound **5**
Formula	$C_{66}H_{42}In_2N_4O_{13}$	$C_{19}H_{13.5}InNO_{5.25}$	$C_{38}H_{27}InN_2O_9$	$C_{76}H_{54}In_2N_4O_{18}$	$C_{76}H_{50}In_2N_4O_{16}$
Temperature/K	295(2)	296(2)	295(2)	295(2)	295(2)
Wavelength/Å	0.71073	1.54178	0.71073	0.71073	0.71073
Molecular weight/g mol^{-1}	1326.66	454.12	770.44	1540.87	1504.84
Crystal system	Triclinic	Monoclinic	Orthorhombic	Triclinic	Triclinic
Space group	$P\bar{1}$	$P2(1)/n$	$P2(1)2(1)2(1)$	$P\bar{1}$	$P\bar{1}$
a/Å	9.835(2)	10.7789(3)	12.8039(9)	9.9495(6)	10.6135(12)
b/Å	13.839(3)	8.2923(2)	14.0375(9)	13.0898(8)	11.6513(13)
c/Å	21.881(5)	19.6538(5)	18.358(1)	13.2297(8)	14.0949(15)
α/°	96.492(4)	90.00	90.00	82.543(1)	75.745(2)
β/°	100.320(5)	95.031(1)	90.00	85.472(1)	68.609(2)
γ/°	104.967(4)	90.00	90.00	80.571(1)	88.736(2)
V/Å^3	2790.5(11)	1749.93(8)	3299.5(4)	1682.4(2)	1568.5(3)
Z	2	4	4	1	1
Flack parameter			0.002(15)		
R indices (all data)	$R_1 = 0.0758$ w$R_2 = 0.2108$	$R_1 = 0.0739$ w$R_2 = 0.2452$	$R_1 = 0.0398$ w$R_2 = 0.0646$	$R_1 = 0.0405$ w$R_2 = 0.0922$	$R_1 = 0.0652$ w$R_2 = 0.1072$

–[InO_5N_2]–, with four In–O bonds coming from chelating carboxylate groups of L1 ligands (L1A and L1B), one In–O bond coming from a monodentate L1 carboxylate group (L1C) and two In–N bonds coming from phenanthroline ligands, which are bonded to In(2) in a η^2 chelate mode. The resultant polyhedron is a monocapped octahedron. This arrangement gives rise to a one-dimensional MOF with formula $[In_2(L1)_3(phen)_2]\cdot H_2O$ (see Fig. 2).

It is remarkable that L1 carboxylate groups show different coordination modes. On one hand, two independent L1 ligands (L1A and L1B) act in a η^2 chelate mode by their two carboxylate groups along the [1 1 0] direction: the L1A ligand connects different In(1) and In(2) ions, while the L1B one links two equivalent In(1) ions. The corresponding torsion angles between the aromatic rings are 58.23° for L1A and 79.57° for L1B. On the other hand, L1C ligand acts in a monodentate η^1 mode by one carboxylate group and in a η^2 chelate mode by the other carboxylate group along the [0 1 $\bar{1}$] direction, connecting two equivalent In(2) ions. The corresponding torsion angle between the aromatic rings is 83.10°.

Hydration water molecules are donors of two H-bond interactions: one water molecule interacts with the monodentate coordinated L1C carboxylate group, while the other one interacts with the L1A carboxylate group bounded to In(2).

Additionally, there are two weak C–H···O interactions, in which the phenanthroline molecule and L1A ligand act as donors, and O atoms of L1A and L1B carboxylate groups act as acceptors.

Compound 2. This compound crystallizes in the monoclinic system, $P2_1/n$ space group. The asymmetric unit is built up from one In(III) ion, one L1 ligand, one hydroxyl group, half 4,4′-bipy molecule and one hydration water molecule. Fig. 1b shows the complete coordination environment of the metal cation.

The In ion is heptacoordinated –[InO_6N]– with four In–O bonds coming from both chelating carboxylate groups of the L1,

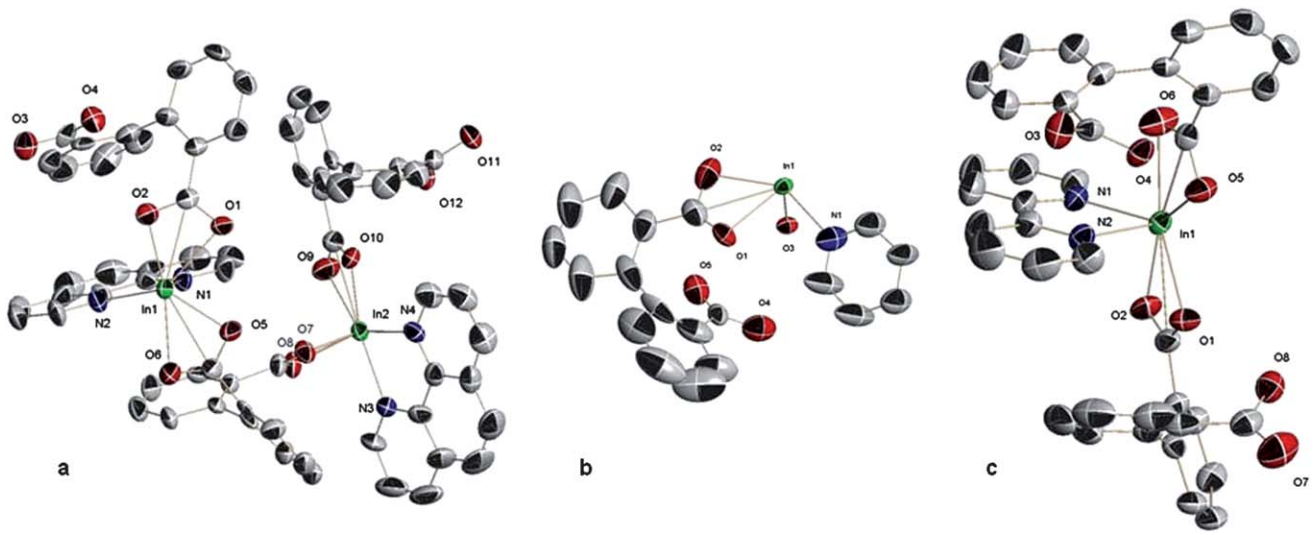

Fig. 1 Coordination spheres of In ions in compounds **1** (a), **2** (b) and **3** (c). (Ellipsoids are displayed at the 50% probability level.)

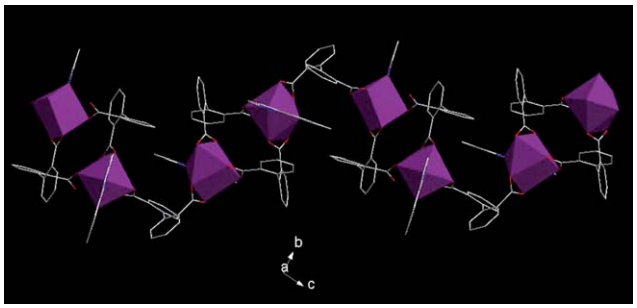

Fig. 2 Perspective view of compound **1** along the [1 0 0] direction.

while the remaining two In–O ones come from two μ-OH groups, generating in this way a coordination polyhedra chain of monocapped octahedra. Besides, the N atoms of the 4,4′-bipy are bounded to the In(III) ion, connecting in this mode the chains giving rise to a layer formation (see Fig. 3). The L1 ligand acts in a chelate mode by its two carboxylate groups, with a torsion angle of −63.65°.

Thus, it connects two adjacent In ions of a chain, which runs in the [0 1 0] direction, while the 4,4′-bipy ligand is located almost perpendicularly to such direction (see Fig. 3). As a result, a zig-zag layer extending parallel to the (0 1 1) plane is built up (see Fig. 3, right). The layers are packed by weak π···π interactions between the aromatic rings of the L1 ligand in neighbour sheets (distance between centroids ≈ 3.88 Å). Moreover, some weak non-covalent interactions OH···C were found, between the water molecule and C_{16} atom of the L_1 aromatic ring, the $O_{100}\cdots C_{16}$ distance being ∼3.11 Å. On the other hand, no H-bond interactions are identified in this structure.

Compound 3. It crystallizes in the orthorhombic system, $P2_12_12_1$ chiral space group. The asymmetric unit consists of one In(III) ion, one L1 ligand, another one partially deprotonated (L2 from now on), one 2,2′-bipy molecule and one hydration water molecule. The In ion is octacoordinated –$[InO_6N_2]$– with four In–O bonds coming from both chelating carboxylate groups of the L1 while the remaining two In–O ones come from the deprotonated carboxylate group of L2 ligand. Besides, the N atoms of the 2,2′-bipy are bounded in a typical chelate mode (Fig. 1c). The resultant polyhedron is a triangulated dodecahedron.

The L1 ligand acts in a η^2 chelate mode by its two carboxylate groups connecting equivalent In(III) ions through a translation in the [1 0 0] direction. This ligand exhibits a torsion angle between aromatic rings of 113.7° and generates helical chains of In–L1–In that extend along the *a* direction (see Fig. 4).

The 2,2′-bipy and the L2 ligand fill the coordination sphere of the In atom and decorate the chains. One of the aromatic rings of the L1 is located almost parallel to one pyridine ring of the 2,2′-bipy, the distance between the centroids being 3.95 Å, according to a weak π···π stacking interaction.

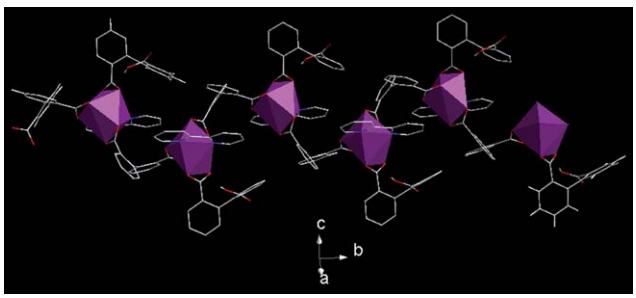

Fig. 4 Perspective view of the helical chain in compound **3**.

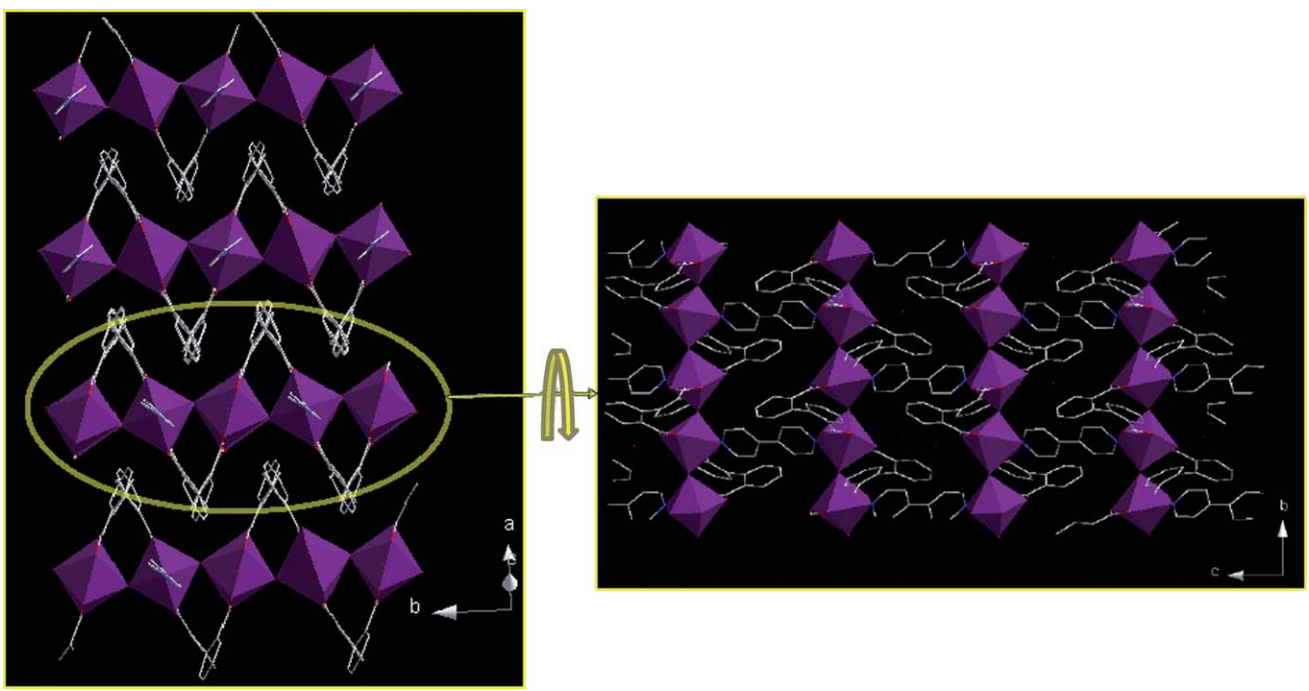

Fig. 3 Perspective views of compound **2** showing a layer (right) and the packing of the layers (left).

The L2 ligand acts in a chelate mode by one carboxylate extreme while the other one remains protonated and without coordination to the In atom. The torsion angle of L2 is −106.9°, which favors the formation of an intramolecular strong H-bond interaction between the protonated group and the deprotonated one, the distance d(O–H···O) ≈ 1.95 Å and α(O–H···O) = 162°.

On the other hand, the hydration water molecule is a donor for two H-bond interactions, one of them to the oxygen atom of the C═O group of the uncoordinated carboxylic extreme of L2, whereas the other is formed with one oxygen atom (O2) of the coordinated carboxylate group of the same ligand.

The previously mentioned strong H-bond interactions could be controlling the crystal and supramolecular structure besides contributing in the stabilization of the network packing.

Additionally, there are two weak C–H···O interactions, in which 2,2′-bipy molecule and L1 act as donors, and O atoms of L2 carbonyl groups act as acceptors. The resultant MOF has a one-dimensional structure, and the chains packing is stabilized by several non-covalent interactions.

Compound 4. This compound crystallizes in the triclinic system, $P\bar{1}$ space group. In the asymmetric unit there are: one In (III) ion, one L1 ligand, one L2 ligand, one phenanthroline molecule and one hydration water molecule. The In ion is octa-coordinated –[InO_6N_2]–. Four In–O bonds come from chelating carboxylate groups of L1 and two In–O bonds are from deprotonated carboxylate group of L2 ligand. Besides, the N atoms of the 2,2′-bipy molecule are bounded in its typical chelate mode (see Fig. 5a). The resultant polyhedron is a triangulated dodecahedron.

In this case, the L1 ligand acts in a η^2 chelate mode by its two carboxylate groups connecting two equivalent In(III) ions (Fig. 6), forming a dimeric unit (square cavity) whose dimensions are about 5.00 × 5.02 Å^2, exhibiting a torsion angle between aromatic rings of 94.92°.

The L2 ligand coordinates metallic centers as chelate by its carboxylate group while its protonated one is uncoordinated. The torsion angle between the aromatic rings is 54.47°. This

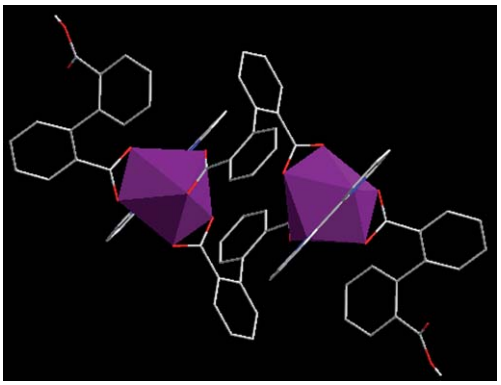

Fig. 6 Perspective view of compound **4** showing a dimeric unit.

conformation leads to the formation of two strong intermolecular H-bond interactions: one between the protonated group and the hydration water molecule (d(O8–H8···O9) ≈ 1.83 Å, α(O8–H8···O9) = 169.1°) and the other between the deprotonated group and the hydration water molecule (d(O9···O2) ≈ 2.83 Å). Moreover, two weak non-covalent OH···C interactions were found, between the water molecule and C35 and C36 atoms of L_1 aromatic ring, the distances of O9–H9WA···C35 being ~2.61 Å and O9–H9WA···C36 ~2.59 Å. Additionally, several C–H···O type interactions are found between the phenanthroline ligand acting as donor and L1 and L2 carboxylate groups.

Compound 5. This compound, which crystallizes in the triclinic system and $P\bar{1}$ space group, has important structural similarities with compounds **3** and **4**, sharing the same contents of the asymmetric unit except by the absence of the hydration water molecule. Another difference with compounds **3** and **4** is that in **5** the In atom is hexacoordinated –[InO_4N_2]–, forming a distorted trigonal prism (see Fig. 5b), while in **3** and **4** it is octacoordinated –[InO_6N_2]–. The L1 ligand, which is completely deprotonated, connects two crystallographically equivalent In atoms forming a dimer, as in compound **4**. This ligand acts as η^2 chelate by one

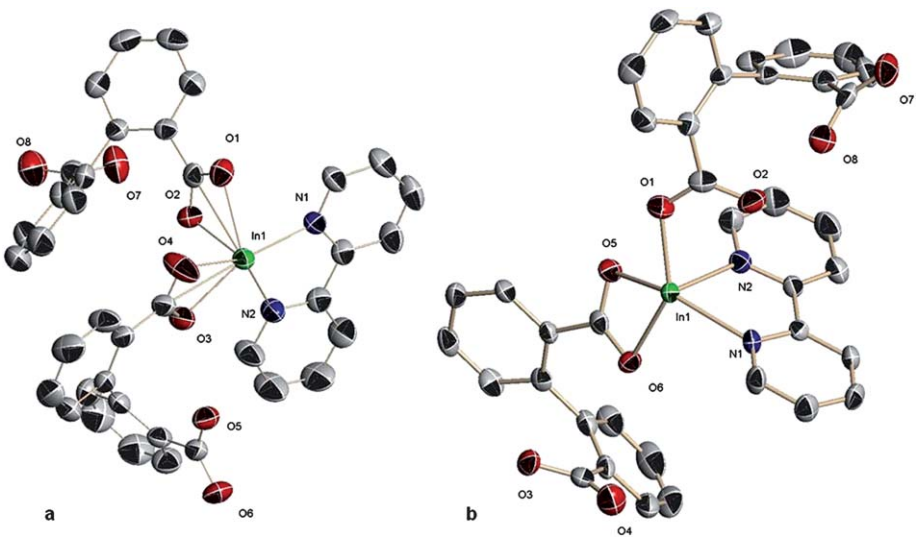

Fig. 5 Coordination spheres of In ions in compounds **4** (a), and **5** (b). (Ellipsoids are displayed at the 50% probability level.)

carboxylate group and as monodentate by the other one. On the other hand, the dihedral angle between aromatic rings in this compound is 74.22°, being in this way the more eclipsed conformation that L1 acquires in **1** to **4** compounds.

The L2 ligand is partially protonated and coordinates in a monodentate mode by its carboxylate group while is uncoordinated by its protonated one. The torsion angle between the aromatic rings is 98.8°.

A square cavity (of smaller size than in compound **4**) is found inside the dimer whose dimensions are about 4.07 × 4.90 Å^2. This slightly different size of the cavity is due to the more closed conformation adopted by L1 in this compound.

On the other hand, the 2,2′-bipy molecules in neighbor dimers are orientated in such way that these small cavities are blocked, which can be observed from the projection of the structure along the *a* direction (see Fig. 7).

In this compound, an intramolecular H-bond interaction is observed again in the partially protonated L2 ligand, but in this case such interaction is stronger than in compounds **3** and **4**, the distance *d*(H···O) being 1.79 Å and the angle *α*(O–H···O) 175.77°. This is the probable cause of the lower value in the torsion angle between aromatic rings in the L2 ligand, which probably means that in this compound L2 exhibits a torsion angle with an optimum value that favors the formation of such interaction. There are also some weak non-covalent interactions, as in the case of compounds **3** and **4**. The 2,2′-bipy molecules disposition results in the existence of a π···π interaction, the distance between its rings being ~3.4 Å. On the other hand, these molecules are donors in two C–H···O interactions to the O atom (O7) of the carboxylic group with a distance *d*(H···O) of 2.57 Å, and to one O atom of the chelate carboxylate group, *d*(H···O) = 2.62 Å.

Topological study

Despite the fact that the obtained In MOFs show 1D and 2D covalent nets, we were interested in studying the supramolecular framework development in order to examine the influence of such interactions in the crystalline packing of these compounds. In this way, we have focused on the H-bond interactions between carboxylate groups and the hydration water molecules, allowing us to explain the supramolecular structural architecture.

Compound 1. Considering the H-bond interactions found by the structural analysis, a new net can be described. Thus, the simplified net of compound **1** results in a binodal layer with 3- and 4-connected nodes shown in Fig. 8a. The resultant network topology has a point symbol $(4.6^2)_2(4^2.6^2.8^2)$.

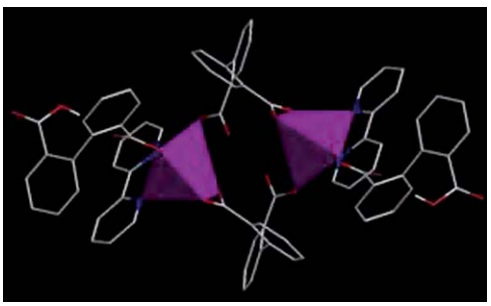

Fig. 7 Perspective view of compound **5** showing a dimeric unit.

Compound 2. In this case, due to the fact that there are no H-bond interactions in the structure, the layers do not extend to a 3D-supramolecular structure. In this way, the resultant most simplified depiction of the covalent 2D framework of compound **2** is a uninodal 3-connected net, which is shown in Fig. 8b. The resultant network topology has a point symbol (6^3) and corresponds to an **hcb** net.

Compound 3. The existence of several H-bond interactions in this compound allows the development of a 3D-supramolecular structure. The simplified net is uninodal, with 4-connected nodes. The resultant network topology has a point symbol (6^6) and corresponds to the **dia** type (Fig. 8c).

Compounds 4 and 5. In the case of compound **4**, the existence of inter-dimer H-bond interactions allows for the development of 1D-supramolecular chains (Fig. 8d). However, compound **5** contains only intra-dimer H-bond interactions avoiding in this way the 1D, 2D or 3D supramolecular structures formation (Fig. 8e). In this way, the crystal packing of dimeric units should be governed by weaker non-covalent interactions.

Thermogravimetric analysis

TGA curves for compounds **1–3** are shown in the ESI, Fig. S4†.

Compound **1** exhibits a weight loss (~1%), which takes place between 100 and 300 °C, corresponding to the loss of the water molecule. This *framework* is stable up to 340 °C with a main sharp process at 450 °C, followed by another minor weight loss up to 500 °C, corresponding to its total decomposition. The final residue at 800 °C is pure In_2O_3 (ICSD_640179), confirmed by XRPD.

The total decomposition of **2** involves three steps. The first one (~2.26%) is the loss of water; the second one (~21.14%) between 300 and 380 °C corresponds to the loss of the 4,4′-bipyridine molecule and the third one (~43.20%) is due to the loss of the carboxylic acid. Finally, the total decomposition of the *framework* at temperatures above 450 °C results in In_2O_3 (ICSD_640179) as a residual solid, confirmed by XRPD.

Compound **3** shows a first weight loss (~1.9%) attributable to the loss of water. Then a second loss (~54.7%) between 300 and 430 °C corresponds to the loss of the diphenic acid and the final loss (~24.8%) is assigned to the departure of the 2,2′-bipyridyl, which entails the total decomposition of the compound into In_2O_3 (ICSD_640179), confirmed by XRPD.

In all cases, the experimental data are in perfect agreement with the theoretical values calculated for the compounds **1–3**.

Infrared spectra

The FTIR spectra of compounds **1–3** are displayed in the ESI, Fig. S5†.

The infrared spectra of compounds **1** and **2** do not show bands attributable to COOH groups, while the bands corresponding to deprotonated carboxylate groups are observed. By contrast,

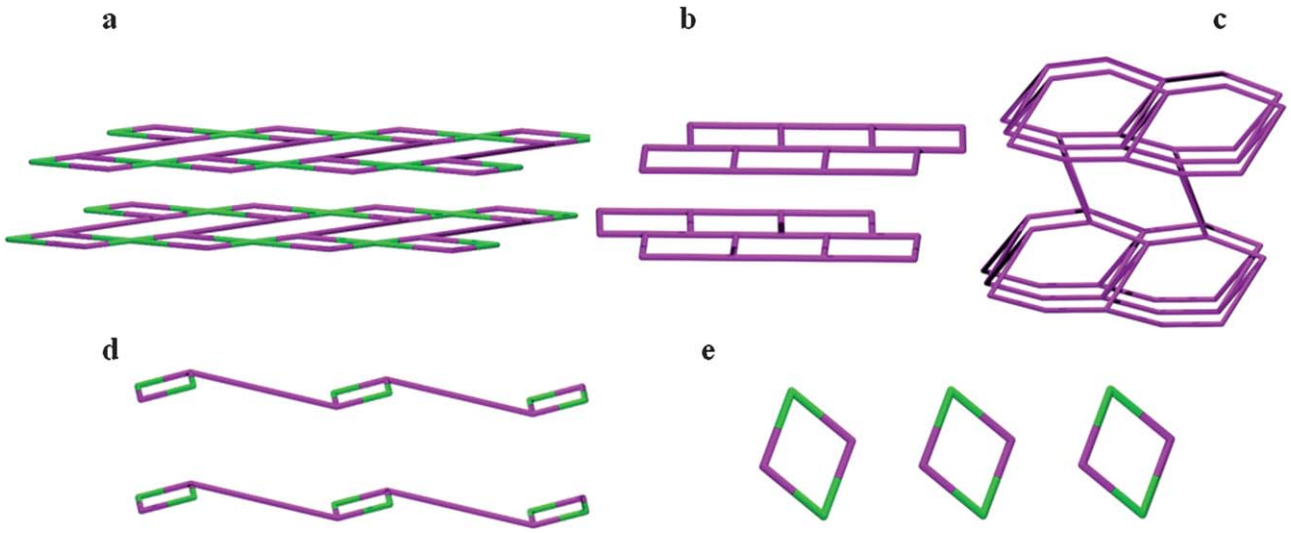

Fig. 8 Topological depictions of compounds: (a) **1**, (b) **2**, (c) **3**, (d) **4** and (e) **5**.

spectrum of **3** clearly shows the bands corresponding to protonated carboxylic groups at 3429 and 3224 for ν(OH) and at 1729 for ν(C═O), together with the bands corresponding to the deprotonated ones, confirming the existence of two types of carboxylic groups. The bands corresponding to the hetero-aromatic ligands are also shifted with respect to the free molecules,[35] confirming they are bonded to the indium ions.

Conclusions

Three In(III) MOFs with diphenic acid were synthesized and obtained as pure phases. Two of them have 1D chain structures (**1** and **3**) and the third (**2**) forms 2D zig-zag layers. Different torsion angles adopted by the diphenic ligand along with the existence of several non-covalent interactions govern the crystal packing and determine the formation of a centrosymmetric one-dimensional compound (**1**) or a non-centrosymmetric helical chain-based compound (**3**).

The replace of the ancillary chelating phenanthroline and 2,2′-bipyridine molecules, which lock two coordination sites of the In coordination environment, by the linear linker 4,4′-bipyridine molecule, leads to obtaining of a 2D-MOF (**2**).

Finally, two additional molecular compounds have been obtained during the synthesis optimization process. Different types of H-bond interactions have been identified in such compounds, which allow us to explain the different crystalline packing and supramolecular chemistry.

Acknowledgements

This work has been supported by the Spanish MCYT Project Mat 2007-60822, CTQ2007–28909-E/BQU, and Consolider-Ingenio CSD2006–2001. AEPP acknowledges JAE fellowship from CSIC and Fondo Social Europeo from EU.

Notes and references

1 J. An, N. L. Geibs and S. Rosi, *J. Am. Chem. Soc.*, 2010, **132**, 38.
2 A. E. Platero Prats, V. A. de la Peña-O'Shea, M. Iglesias, N. Snejko, A. Monge and E. Gutiérrez-Puebla, *ChemCatChem*, 2010, **2**, 147.
3 Q. K. Liu, J. P. Ma and Y. B. Dong, *Chem.–Eur. J.*, 2009, **15**, 10364.
4 V. Finsy, C. E. A. Kirschhock, G. Vedts, G. Maes, L. Alaerts, D. E. De Vos, E. Dirk, G. V. Baron and J. F. M. Denayer, *Chem.–Eur. J.*, 2009, **15**, 7724.
5 F. Millange, N. Guillou, M. E. Medina, G. Férey, A. Carlin-Sinclair, K. M. Golden and R. I. Walton, *Chem. Mater.*, 2010, **22**, 4237.
6 Q. W. Li, W. Y. Zhang, O. S. Miljanic, C. H. Sue, Y. L. Zhao, L. H. Liu, C. B. Knobler, J. F. Stoddart and O. M. Yaghi, *Science*, 2009, **325**, 855.
7 S. Horike, S. Shimomura and S. Kitagawa, *Nat. Chem.*, 2009, **1**, 695.
8 D. Sarma, K. V. Ramanujachary, S. E. Lofland, T. Magdaleno and S. Natarajan, *Inorg. Chem.*, 2009, **48**, 11660.
9 G. Novitchi, W. Wernsdorfer, L. F. Chibotaru, J. P. Costes, C. E. Anson and A. K. Powell, *Angew. Chem., Int. Ed.*, 2009, **48**, 1614.
10 G. S. Papaefstathiou and L. R. MacGillivray, *Coord. Chem. Rev.*, 2003, **246**, 169.
11 Y. Yoshida, K. Inoue and M. Kurmoo, *Inorg. Chem.*, 2009, **48**, 267.
12 S. C. Xiang, W. Zhou, J. M. Gallegos, Y. Liu and B. L. Chen, *J. Am. Chem. Soc.*, 2009, **131**, 12415.
13 C. Volkringer, T. Loiseau, M. Haouas, F. Taulelle, D. Popov, M. Burghammer, C. Riekel, C. Zlotea, F. Cuevas, M. Latroche, D. Phanon, C. Knöfelv, P. L. Llewellyn and G. Férey, *Chem. Mater.*, 2009, **21**, 5783.
14 L. Q. Ma, C. Abney and W. B. Liu, *Chem. Soc. Rev.*, 2009, **38**, 1248.
15 J. Lee, O. K. Farha, J. Roberts, K. A. Scheidt, S. T. Nguyen and J. T. Hupp, *Chem. Soc. Rev.*, 2009, **38**, 1450.
16 N. L. Rosi, M. Eddaoudi, J. Kim, M. O'Keeffe and O. M. Yaghi, *Angew. Chem., Int. Ed.*, 2002, **41**, 284.
17 H. Furukawa, J. Kim, N. W. Ockwig, M. O'Keeffe and O. M. Yaghi, *J. Am. Chem. Soc.*, 2008, **130**, 11650.
18 R.-Q. Zhong, R.-Q. Zou, M. Du, T. Yamada, G. Maruta, S. Takeda, J. Li and Q. Xu, *CrystEngComm*, 2010, **12**, 677.
19 C. Serre, C. Mellot-Draznieks, S. Surblé, N. Audebrand, Y. Filinchuk and G. Férey, *Science*, 2007, **315**, 1828.
20 A. Monge, N. Snejko, E. Gutiérrez-Puebla, M. Medina, C. Cascales, C. Ruiz-Valero, M. Iglesias and B. Gómez-Lor, *Chem. Commun.*, 2005, 1291.
21 F. Gándara, V. A. de la Peña O'Shea, F. Illas, N. Snejko, D. M. Proserpio, E. Gutiérrez-Puebla and M. A. Monge, *Inorg. Chem.*, 2009, **48**, 4707.
22 Y. B. Wang, X. J. Zheng, W. J. Zhuang and L. P. Jin, *Eur. J. Inorg. Chem.*, 2003, 1355.
23 J. Y. Lu and V. Schauss, *Inorg. Chem. Commun.*, 2003, **6**, 1332.
24 S. Hu, J. P. Zhang, H. X. Li, M. L. Tong, X. M. Chen and S. Kitagawa, *Cryst. Growth Des.*, 2007, **7**, 2286.

25 P. D. C. Dietzel, R. Blom and H. Fjellvag, *Dalton Trans.*, 2006, 586.
26 R. Wang, M. Hong, J. Luo, R. Cao and J. Weng, *Chem. Commun.*, 2003, 1018.
27 K. A. Brown, D. P. Martin, R. M. Supkowski and R. L. LaDuca, *CrystEngComm*, 2008, **10**, 846.
28 C. Volkringer, T. Loiseau, N. Guillou, G. Férey and E. Elkaım, *Solid State Sci.*, 2009, **11**, 1507; D. F. Sava, V. Ch. Kravtsov, F. Nouar, L. Wojtas, J. F. Eubank and M. Eddaoudi, *J. Am. Chem. Soc.*, 2008, **130**, 3768; S. Huh, T.-H. Kwon, N. Park, S.-J. Kim and Y. Kim, *Chem. Commun.*, 2009, **33**, 4953; S. Yang, X. Lin, A. J. Blake, G. S. Walker, P. Hubberstey, N. R. Champness and M. Schroeder, *Nat. Chem.*, 2009, **1**, 487; K. C. Stylianou, R. Heck, S. Y. Chong, J. Bacsa, J. T. A. Jones, Y. Z. Khimyak, D. Bradshaw and M. J. Rosseinsky, *J. Am. Chem. Soc.*, 2010, **132**, 4119; Z. Jin, H.-Y. Zhao, X.-J. Zhao, Q.-R. Fang, Q.-R. Long and G.-S. Zhu, *Chem. Commun.*, 2010, **46**, 8612; E. V. Anokhina, M. Vougo-Zanda, X. Wang and A. J. Jacobson, *J. Am. Chem. Soc.*, 2005, **127**, 15000.
29 B. Gómez-Lor, E. Gutiérrez-Puebla, M. Iglesias, M. A. Monge, C. Ruiz-Valero and N. Snejko, *Chem. Mater.*, 2005, **17**, 2568.
30 B. Gómez-Lor, E. Gutiérrez-Puebla, M. Iglesias, M. A. Monge, C. Ruiz-Valero and N. Snejko, *Inorg. Chem.*, 2002, **41**(9), 2429.
31 F. Gándara, B. Gómez-Lor, E. Gutiérrez-Puebla, M. Iglesias, M. A. Monge, D. M. Proserpio and N. Snejko, *Chem. Mater.*, 2008, 72.
32 *Siemens SAINT Data Collection and Procedure Software for the SMART System*, Siemens Analytical X-ray Instruments, Inc., Madison, WI, 1995.
33 *Siemens SHELXTL, Version 5.0*, Siemens Analytical X-ray Instruments Inc., Madison, WI, 1995.
34 *Software for the SMART System V5. 04 and SHELXTL V 5.1*, Bruker-Siemens Analytical X-ray Instrument Inc., Madison, WI, 1998.
35 K. Nakamoto, *Infrared and Raman Spectra of Inorganic and Coordination Compounds*, John Wiley, New York, 1986.

